



## Adsorption of food dye Acid red 18 onto polyaniline-modified rice husk composite: isotherm and kinetic analysis

Mahboobeh Shabandokht<sup>a</sup>, Ehsan Binaeian<sup>b,\*</sup>, Habib-Allah Tayebi<sup>c</sup>

<sup>a</sup>Department of Chemical Engineering, Islamic Azad University, Shahrood Branch, Shahrood, Iran, email: omega\_ohm2008@yahoo.com

<sup>b</sup>Department of Chemical Engineering, Islamic Azad University, Qaemshahr Branch, Qaemshahr, Iran, Tel. +98 11 33209948; email: ehsan.binaeian@yahoo.com

<sup>c</sup>Department of Textile Engineering, Islamic Azad University, Qaemshahr Branch, Qaemshahr, Iran, email: tayebi\_h@yahoo.com

Received 18 November 2015; Accepted 27 March 2016

### ABSTRACT

In this study, the removal of food dye Acid red 18 from aqueous solution by polyaniline/HCl-modified rice husk (polyaniline/HCl-MRH) composite was studied. Properties of synthesized composite were analyzed and confirmed by SEM and FTIR. Results show that Langmuir adsorption isotherm has the best compatibility with the results of experiments. Kinetic analysis using pseudo-first-order model, pseudo-second-order, and the intra-particle diffusion model was carried out. Results also confirmed that adsorption process is compatible with the pseudo-second-order kinetic model. Thermodynamic parameters such as Gibbs free energy changes ( $\Delta G^\circ$ ), Enthalpy changes ( $\Delta H^\circ$ ), and Entropy changes ( $\Delta S^\circ$ ) were calculated. Negative value of  $\Delta G^\circ$  and positive value of  $\Delta H^\circ$  show that adsorption of Acid red 18 on polyaniline/HCl-MRH is a spontaneous process also endothermic.

*Keywords:* Adsorption; Acid red 18; Adsorption isotherm; Adsorption kinetic; Composite

### 1. Introduction

Industries with high water consumption represent the largest producers for pollutants of water. These wastes include colorful combinations. Dyes are one of the main groups of water contaminants. These materials include organic complex compounds that make them resistant to light, washing, and microbial attacks. So they are not decomposed simply. Direct discharge of the industrial polluted wastewaters to the environment normally leads to environmental damage. Moreover, these dyes are probably decomposed to carcinogenic and toxic compounds that have hazard

effects on the humans, aquatic life, and everything in our biosphere. For this reason, the removal of colorful materials from wastewater is considered nowadays. Thus, the contaminated industrial wastewater must be purified before their discharge to minimize the risk of environmental contaminations produced by this polluted wastewater [1,2]. There are different physical, chemical, and biological methods for dye removal from wastewater. However, chemical and biological methods are effective, special equipment and energy are required in this methods. In addition, these methods or techniques often produce lot of byproducts. Among all existing methods, adsorption is preferred more than other methods. So, this preference is considered due to being effective, simple, and low cost [3,4]. If the

\*Corresponding author.

adsorption system is designed correctly, effluents will have a high quality. Activated carbons prepared from wastes are used in many systems as an adsorbent for dye removal from wastewater. This is due to its high adsorption capacity. Although activated carbon as an adsorbent is used so much, its usage is limited because of its high costs. Large numbers of low-cost unconventional materials such as natural materials, biological adsorbents, industrial, and agricultural wastes are proposed for synthesis of adsorbents. Several natural adsorbents have been utilized by researchers for dye removal, namely waste sugar beet pulp [5], degreased coffee bean [6], garlic peel [7], pumpkin seed hull [8], beech wood sawdust [9], biomass fly ash [10], olive pomace [11], orange peel activated carbon [12], potato plant wastes [13], and cotton plant wastes [14]. Activated carbons available in terms of commercial are usually obtained from wood, coconut shell, brown coal, and coal. In addition, every carbonaceous material can be used as a precursor of carbon adsorbents. Many of the byproducts produced from wood and agricultural products can be used as a low-cost and reversible source for the synthesis of activated carbon. These waste materials often have a low economical value and make a problem during discharge. So, changing into activated carbon is the cause of increased value and will decrease the discharging cost of these wastes. There are some reports that show the production of activated carbon from urban rubbishes and industrial byproducts, such as waste shell of walnut [15], PET waste bottles [16], worn out tires, waste materials obtained from rubbishes during fermentation process, and expired newspapers [17]. According to the recent researches, high capability and economic efficiency of activated carbon produced from byproducts have been proved. Juang et al. [18], in their study in 2002 showed that the adsorption capacity of activated carbon produced from bagasse is in the high range (790–1,060 mg/g). The adsorption capacity of carbon depends on raw material features and operation conditions such as decomposition temperature and activation time. There are many factors that affect the adsorption capacity, such as chemical properties of surface, surface charge, and porosity of the surface. Appropriate carbonaceous adsorbents should have high surface area in spite of porous structure. Guo et al. [19] in 2003 showed that the adsorption capacity will not increase with the increase in surface area, necessarily. Acidic and basic features of carbons affect the structure of isotherms. Adsorption capacity also depends on the level of accessibility of pollutants to the inner surface of the adsorbent. The adsorption mechanisms of dyes on the adsorbents are not exactly clear yet. It is because of adsorption complexity that is depending on electrostatic and

non-electrostatic interactions. Rice husk is local agricultural waste produced from rice grinding. Rice husk as a low-cost material often burnt, which produces undesirable environmental effects. Every year, more than 140 million tons of rice husks are produced, and 96% of them are from developing countries [20]. Use of rice husk as an adsorbent not only decreases the effluent problems but also provides high added value such as activated carbon from rice husk. So the use of activated carbon from rice husk has some disadvantages. Chen et al. [21] observed that supplied adsorbent from rice husk due to high content of silica has low surface area. In the present study, polyaniline/HCl-MRH composite that is a new adsorbent was synthesized. Performance of this composite for the removal of Acid red 18 was compared with rice husk activated carbon and polyaniline. Effects of some parameters such as pH, initial dye concentration, adsorbent dosage, contact time, and temperature on the efficiency of dye removal and adsorption capacity were surveyed. Adsorption equilibrium data were assessed by Langmuir, Freundlich, Redlich–Peterson, Temkin, and Dubinin–Radushkevich adsorption isotherms. Kinetic analysis of adsorption process was performed using pseudo-first-order, pseudo-second-order, and the intra-particle diffusion models. Thermodynamic parameters such as Gibbs free energy ( $\Delta G^\circ$ ), enthalpy ( $\Delta H^\circ$ ), and entropy ( $\Delta S^\circ$ ) were investigated.

## 2. Experimental

### 2.1. Materials

Aniline ( $C_6H_5NH_2$ ), which is an aromatic amine was used for supplying polymers and was purchased from Merck. Acid red 18 was supplied by Dystar Company and was used without any purification. Specifications and structure of Acid red 18 are shown in Table 1 and Fig. 1, respectively.

Rice husk that contains cellulose ( $C_6H_{10}O_5$ )<sub>n</sub> was obtained from north of Iran.  $KiO_3$  as an oxidizer, CTAB as a surfactant, Hexadecyl trimethyl ammonium bromide ( $C_{19}H_{42}BrN$ ), HCl, NaOH,  $H_2SO_4$ ,  $NaHCO_3$ , and  $Na_2CO_3$  were purchased from Merck, Germany.

### 2.2. Preparation HCl-MRH adsorbent sample

About 20 g of rice husk containing cellulose with mesh of 50 were supplied and were stirred with 200 mL of HCl. It was carried out under the reflux for 3 h at 70°C. Then, the prepared sample were filtered, washed with deionized water, and dried for 24 h under vacuum at 60°C. Then the prepared sample was neutralized with 2% solution of  $Na_2CO_3$ , pH of the solution was adjusted at 7.5. After neutralization, the sample was dried for 3 h in 110°C and screened with mesh of 200.

Table 1  
Specifications of Acid red 18

Cas number	CI. number	Formula	Molecular weight	$\lambda_{\max}$
2611-82-7,604.48	16255	$C_{20}H_{11}N_2Na_3O_{10}S_3$	879.86 g/mol	523 nm

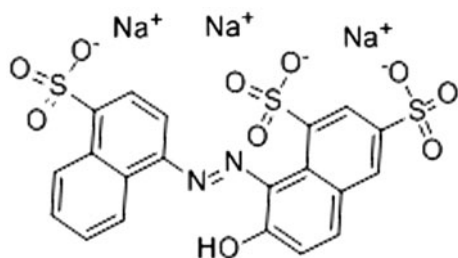


Fig. 1. Chemical structure of Acid red 18.

### 2.3. Preparation of polyaniline

For preparation of polyaniline, 1 g of potassium iodate ( $KIO_3$ ) was added to 100 ml of sulfuric acid 1 M and the solution was stirred by magnetic stirrer for 3 min. Then, 0.2 g of CTAB surfactant was added to the solution. After 20 min, 1 ml of aniline monomer was poured into the solution that caused color change from light violet to dark. This color change indicates the conversion of aniline monomer to the polymer. This reaction carried out under environmental temperature for 5 h. Finally, the product was filtered and impurities (oligomers) were removed. Prepared polyaniline was washed with distilled water and acetone several times and finally was put in the oven for 24 h at 70°C.

### 2.4. Preparation of polyaniline/HCl-MRH composite

For preparation of composite, 1 g of potassium iodate ( $KIO_3$ ) was added to 100 ml of sulfuric acid 1 M and the solution was stirred by magnetic stirrer for 3 min. Then, 0.2 g of CTAB surfactant and 1 g of HCl-MRH were added to the solution. After 20 min, 1 ml of distilled aniline monomer was poured into the solution that caused color change from light violet to dark. This color change indicates the conversion of aniline monomer to the polymer. This reaction was carried out under environmental temperature for 5 h. Finally, the produced sample was filtered and impurities (oligomers) were removed. Prepared composite was washed with distilled water and acetone several times and finally was put in the oven for 24 h. The oven temperature was set at 70°C. After

drying, polyaniline/HCl-MRH composite was ground in a glass mortar and was screened in the sieve with mesh of 200.

### 2.5. Characterization of the adsorbent samples

In order to analyze the structure of synthesized adsorbents, Fourier transform infrared spectroscopy (FTIR) and scanning electron microscope (SEM) were used. Sample surface morphologies were analyzed by a HITACHI S-4160 scanning electron microscopy (SEM). The presence of polyaniline on the structure of the composite was recorded by FTIR analysis (FTIR, 8400S, Shimadzu, Japan) in the wave numbers ranging from 4,000 to 500  $cm^{-1}$  using KBr technique.

### 2.6. Batch adsorption experiments

Batch experiments were carried out in a 250-mL Erlenmeyer flask containing 50 mL of dye solutions for initial concentrations of 40, 60, 80, 100, and 120  $mg L^{-1}$ . Dye solutions were prepared in phosphate buffer of 0.1 M. The experiments were performed under varying pH (3–11) and adsorbent dose (0.04–0.20 g). The pH of the solution was adjusted using 1.0 M HCl and NaOH. To investigate the effect of temperature, adsorption of Acid red 18 on three adsorbents in the temperature ranges of 25 up to 45°C, initial dye concentration of 40 up to 120 ppm, 0.1 g of composite, 0.12 g of polyaniline, and 0.16 g of HCl-MRH at equilibrium time was studied. After adsorption, for each concentration and after 15, 30, 45, 60, 90, 120, and 180 min of contact times, the treated solution was centrifuged by a Kokusan Ensinkico centrifuge apparatus at 5,000 rpm for 30 min. The concentration of dye solutions was measured using ultraviolet-visible spectrophotometer (6310, JENWAY, UK) prior and after adsorption process.  $q_e$  and  $q_t$  were obtained through the following relationships:

$$q_e = (C_i - C_e) \times V/M \quad (1)$$

$$q_t = (C_i - C_t) \times V/M \quad (2)$$

where  $q_e$  and  $q_t$  (mg/g) are the amounts of substance adsorbed at the equilibrium and any time  $t$ ,  $C_i$ ,  $C_e$ , and

$C_i$  (mg/L) are dye concentrations at initial, equilibrium, and any time,  $V$  and  $M$  are the volume of dye solution (L) and the mass of adsorbent (g), respectively. The removal efficiency was also calculated as follows:

$$\text{Removal efficiency (\%)} = (C_i - C_f)/C_i \times 100 \quad (3)$$

where  $C_i$  and  $C_f$  are the initial and final concentrations of dye, respectively.

### 3. Results and discussion

#### 3.1. Characterization of prepared adsorbents

Using spectrum of FTIR, useful information about structure of polyaniline (Fig. 2(a)), HCl-MRH (Fig. 2(b)) and polyaniline/HCl-MRH composite (Fig. 2(c)) was obtained. As can be seen in Fig. 2(a), peaks at 1,494.10, 1,551.86, 1,603.97, and 1,649.13  $\text{cm}^{-1}$  are representative of stretching vibration of C=C in benzene ring, peak at 1,300.78  $\text{cm}^{-1}$  is about stretching vibration of C–N, peaks at 1,391.98  $\text{cm}^{-1}$  and 805.43  $\text{cm}^{-1}$  are showing bending in-plane and bending out-of-plane vibrations of C–H, respectively. Vibration of N–H group at 3,230.14 and 3,471.00  $\text{cm}^{-1}$  is observable [22]. As can be seen in FTIR spectrum of HCl-MRH (Fig. 2(b)), the peaks at 3,382.70 and 3,765.06  $\text{cm}^{-1}$  show stretching vibration of hydroxyl group of carbon and absorbed water on the surface, respectively. Also, the peak at 2,918.75  $\text{cm}^{-1}$  is related to stretching vibration of C–H. Comparison of the FTIR spectra of polyaniline/HCl-MRH composite (Fig. 2(c)), polyaniline (Fig. 2(a)), and HCl-MRH (Fig. 2(b)) shows that in spite of the presence of polyaniline vibration, there is no effect of hydroxyl group vibrations, proving that HCl-MRH was loaded by polyaniline [23].

Fig. 3 shows SEM images of synthesized adsorbents. These images show the morphologies of the particles and confirm that the prepared adsorbents are irregular and porous. Particle size distribution according to SEM images is in the range of 50–100 nm. According to Fig. 2(a) and (b), it can be recognized that the prepared composite is uniform.

#### 3.2. Effect of pH

The effect of pH on the removal of Acid red 18 by composite, HCl-MRH, and polyaniline in the range of 3–11 is investigated and shown in Fig. 4. As can be seen, the maximum removal of dye occurred at pH 3 and according to the dye being anionic, this trend is expected. Since the adsorbent surface is positively charged at lower pH values, the strong electrostatic

attraction between the positive charges of the adsorbent and the negative charges of dye molecules leads to the maximum adsorption of dye. If the pH increases, the number of negative charges of the sites increase and positive charges decrease, so the electrostatic repulsion of negatively charged polyaniline and molecules of anionic dye leads to lower adsorption of dye [24]. The low adsorption of Acid red 18 in alkaline environment is due to the competition between  $\text{OH}^-$  ions and anionic dye molecules to be adsorbed on the sites. Experiments were carried out at 25°C, 0.1 g of adsorbents, initial dye concentration of 40 ppm, and contact time of 120 min.

#### 3.3. Effect of adsorbent dosage

To investigate the effect of adsorbent dosage, 0.02–0.2 g of different adsorbents were examined for 120 min with 40 ppm of dye solution. The percentage of dye removal for three different types of the adsorbents is shown in Fig. 5. As seen, synthesized composite showed the highest efficiency in comparison with the other two adsorbents and more than 0.1 g of composite dosage, no changes have been observed in the dye removal efficiency. So 0.1 g of composite was used in subsequent experiments. Due to well-distributed amine-functionalized groups on the surface of HCl-MRH, the numbers of amine groups per unit area of HCl-MRH will increase, leading to increase in adsorption capacity of composite in comparison with polyaniline and HCl-MRH. The optimum dosage of polyaniline and HCl-MRH were 0.12 and 0.16 g, respectively. At these dosages, no changes in dye removal were observed.

#### 3.4. Effect of contact time

To study the effect of contact time, experiments were carried out in the range of, 40 up to 120 ppm of dye solutions, contact times of 0–180 min, 0.1 g of composite, and pH of 3. As seen in Fig. 6, almost after 120 min, dye adsorption on the surface of composite will reach the equilibrium state. So, 120 min of contact time was considered as an equilibrium time. The aggregation of dye molecules occurs on the surface of composite with an increase in the contact time. So, deeper penetration of dye into the sites having higher energies is impossible. The rest of experiments were considered for 120 min of contact time. The individual, smooth, and continuous adsorption curves show the saturation state and indicate monolayer covering of adsorbent surface by dye molecules [25].

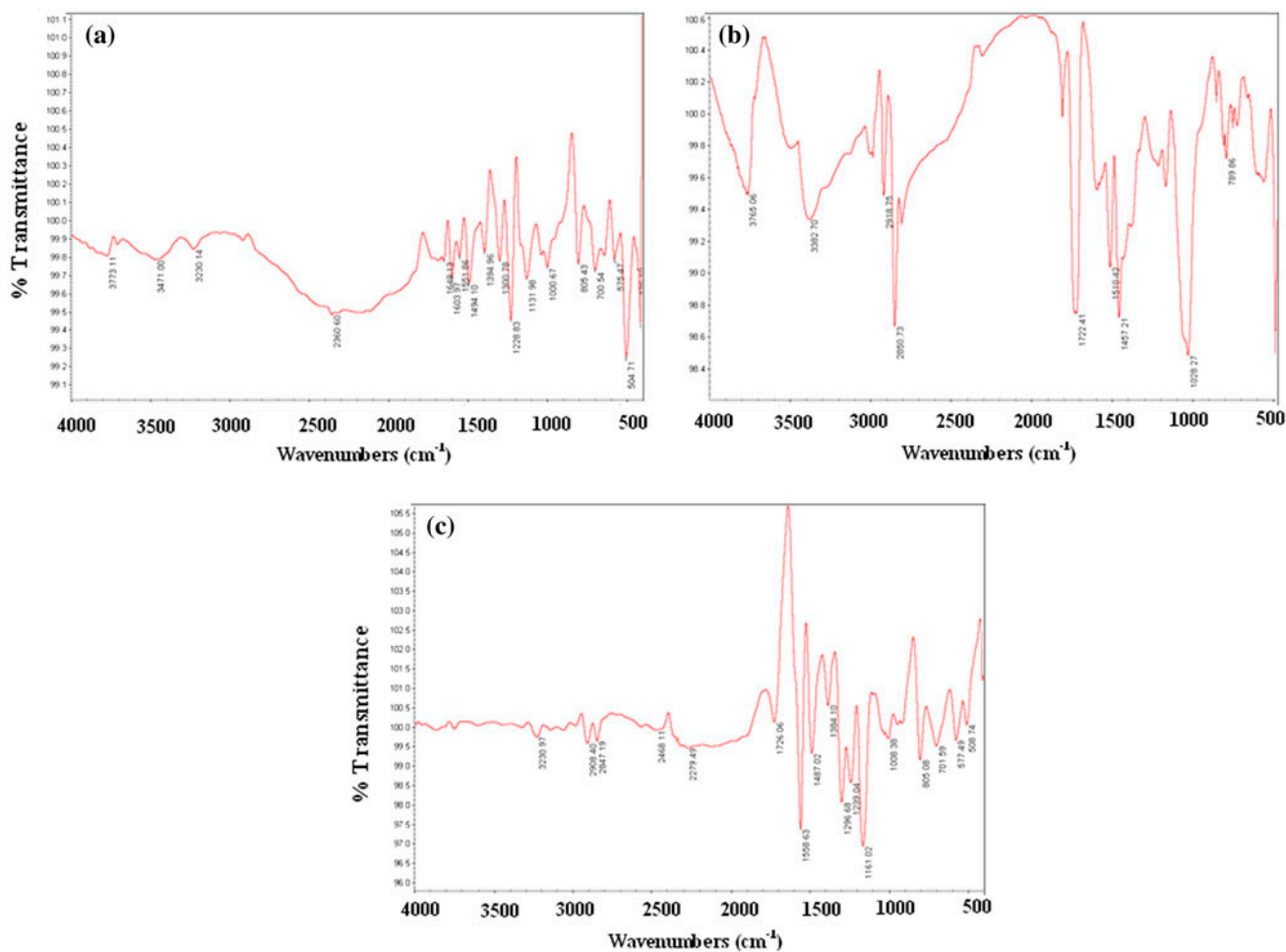


Fig. 2. FTIR spectra of polyaniline (a), HCl-MRH (b), and polyaniline/HCl-MRH composite (c).

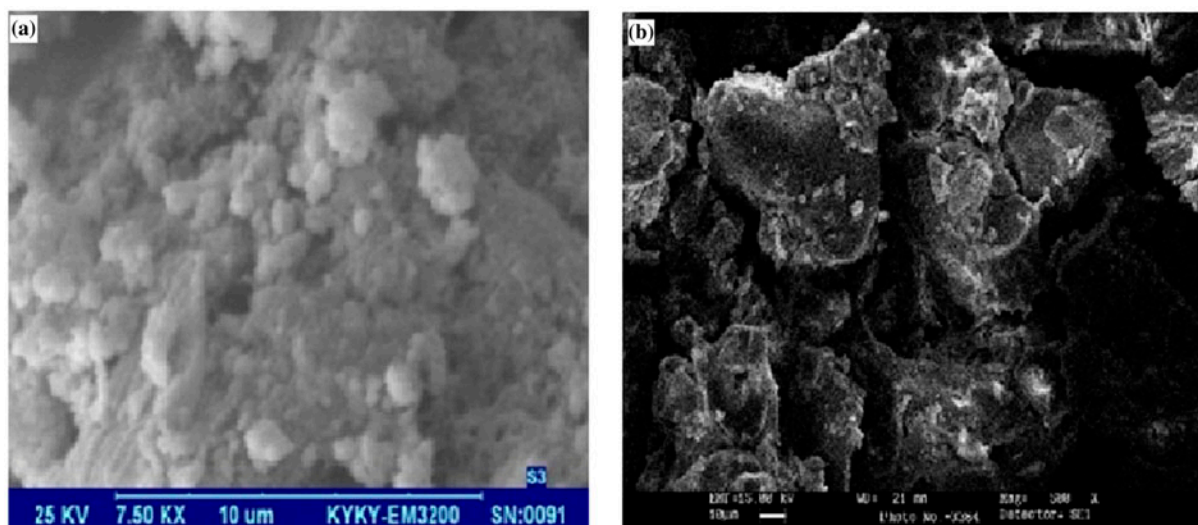


Fig. 3. SEM images of HCl-MRH (a) and polyaniline/HCl-MRH composite (b).

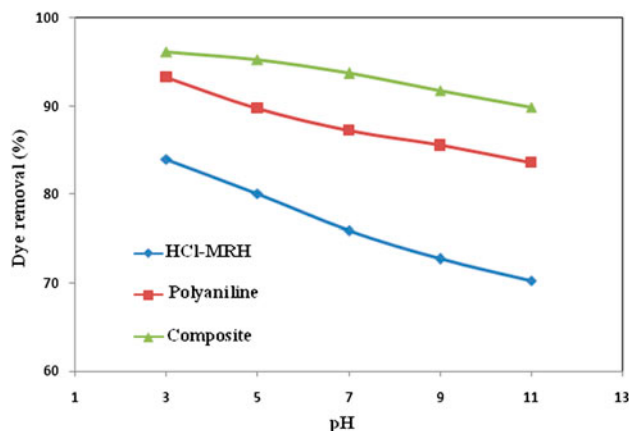


Fig. 4. Effect of pH on Acid red 18 removal (0.1 g of adsorbents, temperature of 25°C, initial dye concentration of 40 ppm, and 120 min contact time).

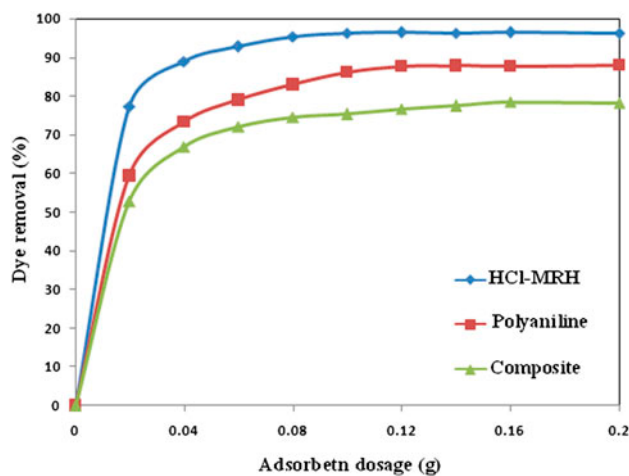


Fig. 5. Effect of adsorbent dosage on percentage of dye removal (initial dye concentration of 40 ppm, contact time 120 min, and pH 3).

### 3.5. Effect of dye concentration

As can be seen in Fig. 7, with the increase in initial dye concentration from 40 up to 120 ppm, dye removal percentage will decrease, while adsorption capacity will increase. Initial dye concentration supplies the required driving force for overcoming mass transfer resistance between liquid and solid phases. Increase in the initial dye concentration also improves the interactions between dye and adsorbent [26,27].

### 3.6. Effect of temperature

The effect of temperature on the adsorption of Acid red 18 onto three adsorbents is shown in Fig. 8.

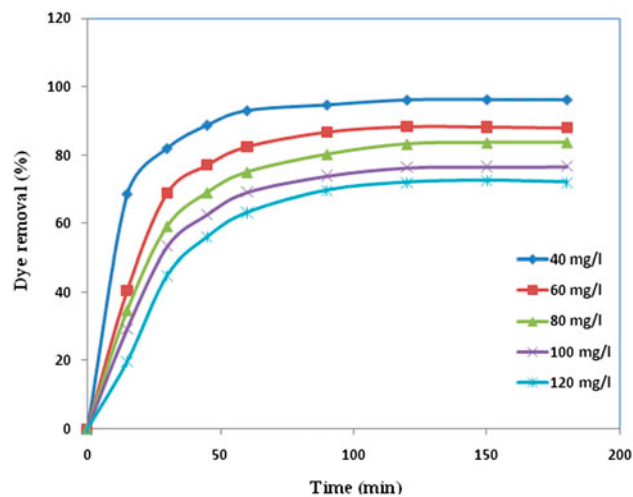


Fig. 6. Effect of contact time on the percentage of dye removal (initial dye concentration of 40 up to 120 ppm, adsorbent dosage of 0.1 g in 50 mL of dye solutions, and pH 3).

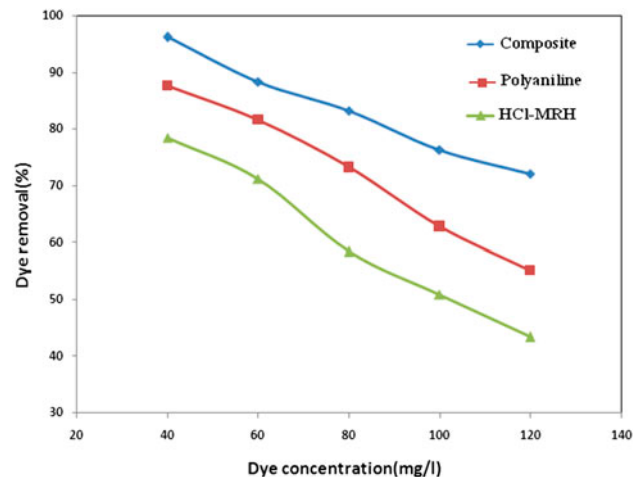


Fig. 7. Effect of initial dye concentration on the percentage of dye removal (initial dye concentration: 40 up to 120 ppm, 0.1 g of composite, 0.12 g of polyaniline, 0.16 g of HCl-MRH, contact time of 120 min).

As can be seen in Fig. 8, with the increase in temperature, efficiency of composite and polyaniline for the removal of dye is increased, while the efficiency of HCl-MRH adsorbent is independent of temperature. It is because of the presence of functional groups on the surface composite. Between three adsorbents, composite exhibited the highest efficiency for dye removal. Also, Fig. 9 shows the effect of initial dye concentrations at different temperatures for the removal of Acid red 18 by composite. It is obvious that the increase in

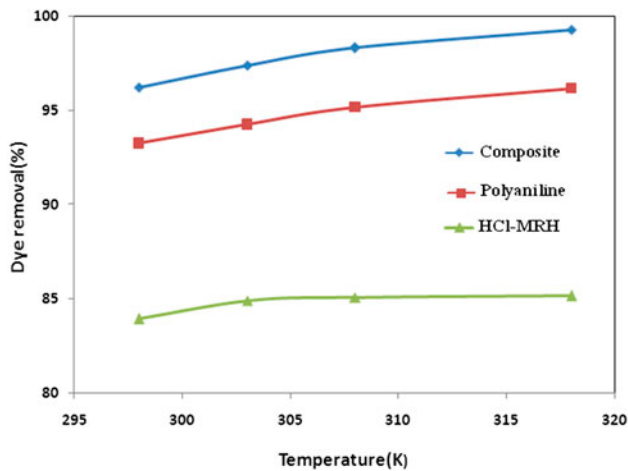


Fig. 8. Effect of temperature on dye removal percentage.

temperature at all ranges of concentrations causes the increase in dye removal. This is due to the increase in surface activity, that shows the adsorption of Acid red 18 on the surface of composite is the endothermic process [26,27].

### 3.7. Thermodynamic studies

Thermodynamic parameters such as  $\Delta G^\circ$ ,  $\Delta H^\circ$ , and  $\Delta S^\circ$  could be calculated by the following equations [24,28]:

$$K_c = C_{Ac}/C_e \quad (4)$$

$$\Delta G^\circ = -RT \ln k_c \quad (5)$$

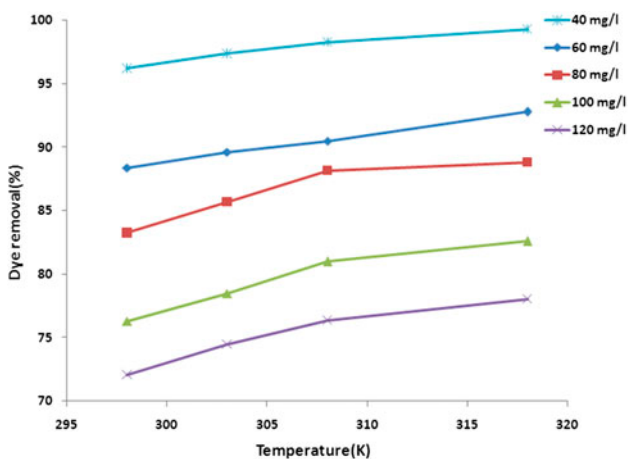


Fig. 9. Effect of temperature on adsorption of dye on composite in different Acid red 18 concentrations.

$$\Delta G^\circ = \Delta H^\circ - T\Delta S^\circ \quad (6)$$

$$\log k_c = \Delta S^\circ / 2.303 R - \Delta H^\circ / 2.303 RT \quad (7)$$

In these equations,  $k_c$ ,  $C_e$ , and  $C_{Ac}$  are the equilibrium constant, the equilibrium concentration in solution (mg/L), and adsorbed dye on the adsorbent in the equilibrium state, respectively.  $\Delta G^\circ$ ,  $\Delta H^\circ$ , and  $\Delta S^\circ$  are the changes in Gibbs free energy, enthalpy, and entropy, respectively. The values of  $\Delta H^\circ$  and  $\Delta S^\circ$  could be calculated from the slope and intercept of the plot of  $\log k_c$  vs.  $1/T$  (Eq. (7)), as shown in Fig. 10.  $\Delta G^\circ$  could be calculated from Eq. (6). It is clear that the adsorption of Acid red 18 on composite sample was enhanced with the increase in temperature from 298 K up to 318 K. So, the adsorption was endothermic. The values of thermodynamic parameters ( $\Delta G^\circ$ ,  $\Delta H^\circ$ ,  $\Delta S^\circ$ ) at different temperatures and different initial concentrations are shown in Table 2. Negative values of  $\Delta G^\circ$  indicate that the adsorption process is feasible and spontaneous. As Table 2 shows, with the increase in temperature, Gibbs free energy becomes more negative and it shows that the increase in temperature promotes the spontaneity of the adsorption process. However, an increase in the initial dye concentration could lower the Gibbs free energy, which is an indication of the fall in the spontaneous adsorption process. The positive values of the  $\Delta H^\circ$  indicate that the adsorption is endothermic. Hence, the magnitude of the heat of adsorption ( $\Delta H^\circ$ ) could describe the type of adsorption.

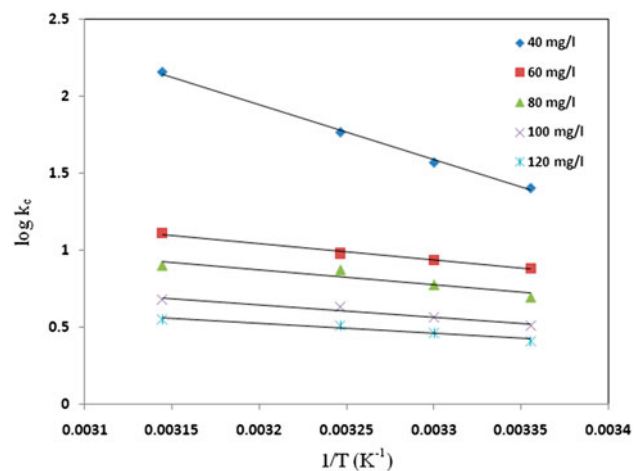


Fig. 10. Effect of temperatures in the range of 25–45°C on the thermodynamic parameters (initial dye concentration: 40–120 ppm, composite dosage of 0.1 g, pH 3, and contact time of 120 min).

Table 2

Thermodynamic parameters for adsorption of Acid red 18 onto polyaniline/HCl-MRH composite

Initial dye concentration (mg/l)	$\Delta H^\circ$ (kJ/mol)	$\Delta S^\circ$ (J/mol K)	$\Delta G^\circ$ (kJ/mol)			
			25°C	30°C	35°C	45°C
40	68.45	256.065	-7.854	-9.138	-10.418	-12.979
60	20.73	86.353	-5.003	-5.435	-5.867	-6.730
80	18.59	76.186	-4.113	-4.494	-4.875	-5.637
100	15.392	61.577	-2.958	-3.266	-3.573	-4.189
120	12.474	49.974	-2.418	-2.668	-2.918	-3.418

The process of adsorption may be physical or chemical. Involved forces in physical adsorption process are weak. So, heat of adsorption usually is not more than 21 kJ/mol. In chemical adsorption, involved forces are more powerful than physical adsorption and heat of adsorption in chemical adsorption is such as heat of chemical reactions about 21–42 kJ/mol [24,26]. According to the obtained values of  $\Delta H^\circ$ , the adsorption of Acid red 18 onto polyaniline/HCl-MRH composite is physical adsorption. Also, the mean adsorption energy ( $E$ ) calculated from D-R model was found to be in the range of 0.9–4 kJ/mol (2,672.61 J/mol), which are in the energy range of physical adsorption reactions [29]. The values of  $\Delta S^\circ$  were applied to describe the randomness of Acid red 18 adsorption process in the adsorbent–solution interface. A positive value of  $\Delta S^\circ$  exhibits an increase in the irregularities in the interface of solution–adsorbent during the adsorption process, which implies an improvement of the efficiency. The changes in positive values of entropy and enthalpy for the adsorption of many dyes onto different adsorbents have been reported in many literatures [25,30].

### 3.8. Equilibrium studies of adsorption

Adsorption isotherms are a major issue and play an important role in determination of maximum adsorption capacity. Adsorption isotherms indicate the effectiveness of the adsorbent during adsorption process and provide possibility of economic assessment of commercial applications of adsorbent for the removal of some specific solutes. For this reason, Temkin, Dubinin–Radushkevich, Redlich–Peterson, Freundlich, and Langmuir isotherms were applied. Parameters of each isotherm were calculated using linear regression and are presented in Table 3.

Compatibility between the experimental data and the results of models could be ranked according to  $R^2$  values as follows:

Langmuir > Freundlich > Redlich–Peterson > Temkin > Dubinin–Radushkevich. For Langmuir isotherm, four kinds of linear regression were used, and the first kind was better matched with the experimental data and has the highest value of  $R^2$  in comparison with three other linear models. Langmuir model is used to determine the value of adsorption capacity.  $q_m$  value signifies the maximum adsorption capacity of the adsorbent (mg/g). Also, the Langmuir constant ( $k_L$ ) is a coefficient that correlates the adsorbent to the adsorbate. High amounts of  $k_L$  values indicate the binding affinity for dye molecules. Freundlich isotherm model is based on experimental data in the nature and is available for heterogeneous surfaces [31]. Freundlich model exhibits that energy of adsorption decreases exponentially on the active sites of an adsorbent. Constant of Freundlich isotherm,  $k_f$ , is used for relative evaluation of the adsorption capacity ( $L g^{-1}$ ). Constant  $n$  shows adsorption intensity and  $1/n$  is the heterogeneity factor of the surface. High values of  $k_f$  express readily the adsorption of dye molecules from aqueous solutions and high values of  $n$  indicate suitable and desirable adsorption. The value of  $n$  below unity shows that adsorption is a chemical process. If the value of  $n$  is equal to unity, the adsorption is linear. The values of  $n$  in the range of 2–10 suggest a favorable and physical adsorption. As can be seen in Table 3,  $n$  value obtained from linear regression is 3.95 showing desired adsorption. The correlation coefficient of Redlich–Peterson isotherm that is a combination of Langmuir and Freundlich isotherms is 0.985 which was smaller than that of Langmuir isotherm. So the Langmuir isotherm is also dominant isotherm. Dubinin–Radushkevich isotherm was evaluated and its correlation coefficient was 0.923, is also lower than that of Langmuir isotherm. In order to study multilayer adsorption on the surface of composite, Temkin isotherm was examined. Correlation coefficient of Temkin isotherm was calculated about 0.982 that is lower than the correlation coefficient of Langmuir model, indicates monolayer adsorption occurred on

Table 3  
Values of parameters for each isotherm model

Isotherm model	Isotherm equation	Linear form of isotherms	$R^2$
Langmuir	$q_e = q_m K_L C_e / (1 + K_L C_e)$	1: $C_e/q_e = K_1/q_m + (1/q_m) C_e$ $C_e/q_e$ vs. $C_e$ $q_m = 100.00, K_1 = 4.30$	0.999
		2: $1/q_e = K_L/q_m C_e + 1/q_m$ $1/q_e$ vs. $1/C_e$ $q_m = 76.92, K_1 = 1.54$	0.902
		3: $q_e = q_m - (K_L) q_e/C_e$ $q_e$ vs. $q_e/C_e$ $q_m = 78.62, K_1 = 1.70$	0.783
		4: $q_e/C_e = q_m/K_1 - q_e/K_1$ $q_e/C_e$ vs. $q_e$ $q_m = 32.82, K_1 = 1.90$	0.559
Freundlich	$q_e = K_f C_e^{1/n}$	$\ln q_e = \ln K_f + 1/n \ln C_e$ $\ln q_e$ vs. $\ln C_e$ $n = 3.95, K_f = 33.98$	0.992
Redlich–Peterson	$q_e = k_R C_e / (1 + \alpha_R C_e^\beta)$	$\ln(K_R \times (C_e/q_e) - 1)$ vs. $b \ln C_e + \ln a_R$ $K_R = 22, \alpha_R = 0.325, \beta = 0.907$ $K_R$ was calculated by trial and error	0.985
Temkin	$q_e = B \ln(AC_e)$	$q_e$ vs. $\ln C_e$ $B = 13.63$ $A = 12.16$	0.982
Dubinin–Radushkevich	$q_e = q_{m,exp.} (-K_{ads} \epsilon^2)$	$\ln q_e$ vs. $(\ln(1 + 1/C_e))^2$ $q_m = 116.00$ mg/g $K_{ads} = 7e-8$ mg/l $E = 1/(\sqrt{2\beta}) = 2672.61$ J/mol	0.923

the surface of composite [32,33]. The dimensionless parameter  $R_L$  in the Langmuir isotherm is one of the effective parameters that is expressed by the following equation [33]:

$$R_L = 1/(1 + bC_0) \quad (8)$$

where  $C_0$  and  $b$  are the initial dye concentration and Langmuir constant, respectively. The type of adsorption, which is classified according to the values of  $R_L$ , is listed in Table 4.

The values of  $R_L$  for the Langmuir isotherm are shown in Table 5. As can be seen in Table 5,  $R_L$  values are between 0 and 1. So, according to the Table 4, the adsorption of Acid red 18 onto the composite is a favorable process. As can be seen, for whole linear models of Langmuir isotherm, adsorption of Acid red 18 on composite is favorable. For comparative purposes, the adsorption capacity of food dyes onto different adsorbents is also listed in Table 6. The results in Table 6 show that the polyaniline/HCl-MRH composite has a large adsorption capacity. This was due to the presence of high amounts of amine groups of polyaniline.

Table 4  
Effect of  $R_L$  values on adsorption quality

Adsorption quality	$R_L$
Unfavorable adsorption	$R_L > 1$
Favorable adsorption	$0 < R_L < 1$
Irreversible adsorption	$R_L = 0$
Linear adsorption	$R_L = 1$

### 3.9. Adsorption kinetics

The study of adsorption kinetics is a very important factor in the investigation of adsorption. In order to predict adsorption mechanism and determining controlling steps such as mass transfer and chemical reaction kinetic models were used. To determine the rate of dye adsorption on the surface of rice husk, kinetic models of intra-particle diffusion, pseudo-first-order, and pseudo-second-order were investigated. These models contain whole levels of adsorption such as outer film penetration, adsorption, and particle penetration. So they are sample model (like model). Kinetic pseudo-first-order model for reversible reactions that is between equilibrium solid or liquid is

Table 5

Values of  $R_L$  for the adsorption of Acid red 18 on composite at 298 K and different initial concentrations

Langmuir isotherm	$R_L$				
	40 ppm	60 ppm	80 ppm	100 ppm	120 ppm
Linear type 1	0.006	0.004	0.003	0.002	0.002
Linear type 2	0.016	0.010	0.008	0.006	0.005
Linear type 3	0.014	0.010	0.007	0.006	0.005
Linear type 4	0.013	0.007	0.007	0.005	0.004

Table 6

Adsorption capacities for the removal of food dyes by different adsorbents

Adsorbent	$q_m$ (mg/g)	pH	Concentration range (mg/L)	Refs.
Amberlite FPA51	131	4.87	100–1,500	[34]
Mangrove bark	12.7	2	–	[35]
Cd(OH) <sub>2</sub> -NW-AC	76.9	1	50–200	[36]
Ag-NP-AC	37.0	1	50–200	[36]
Polyaniline/HCl-MRH	100	3	40–120	This study

Notes: AC: activated carbon; NW: nanowires; NP: nanoparticles; MRH: modified rice husk.

used, while in pseudo-second-order model it was assumed that speed limiter level may be chemical adsorption. In pseudo-first-order model, speed of adsorbent active sites that is occupied is proportional to the numbers of empty sites, while in pseudo-second-order model controller level of adsorption speed contains capacity forces that were done through sharing or changing electrons between adsorbent and adsorbate.

### 3.9.1. The pseudo-first-order kinetic model

Pseudo-first-order model was suggested by Lagergren. This model is expressed using the following equation [37]:

$$\ln(q_e - q_t) = \ln(q_e) - k_{ad}t \quad (9)$$

In the Lagergren pseudo-first-order model,  $q_e$  (mg g<sup>-1</sup>) and rate constant  $k_{ad}$  (min<sup>-1</sup>) were calculated at different concentrations from the plot of  $\ln(q_e - q_t)$  vs.  $t$  as shown in Fig. 11. The findings are listed in the Table 7.

The correlation coefficients of pseudo-first-order model are lower than that of the pseudo-second-order. In addition, the significant difference between experimental and calculated values of equilibrium adsorption capacity ( $q_e$ ) was observed that shows the experimental data are not compatible with the pseudo-first-order kinetic model.

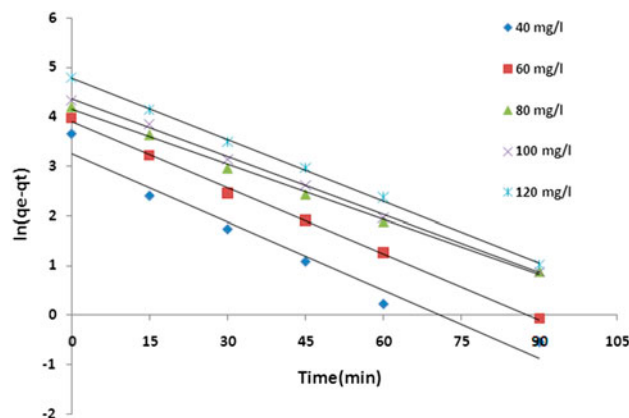


Fig. 11. Pseudo-first-order kinetic model for adsorption of Acid red 18 onto the composite at 25°C.

### 3.9.2. The pseudo-second-order kinetic model

Pseudo-second-order kinetic model of Ho has also been investigated which is given by the following equation [37]:

$$t/q_t = 1/k_h q_e^2 + t/q_e \quad (10)$$

From the plot of the values of  $t/q_t$  vs.  $t$  and as shown in Fig. 12, straight lines are obtained where the values of  $q_e$  and  $k_h$  could be estimated from the

Table 7

Comparison of the constants of pseudo-first-order, pseudo-second-order, intra-particle diffusion kinetic models, experimental, and calculated values of  $q_e$  at different initial concentrations of Acid red 18

Initial DY86 concentration (mg/L)	Pseudo-first-order			Pseudo-second-order			Intra-particle diffusion			
	$k_{ad}$ (min <sup>-1</sup> )	$q_e$ (mg/g)	$R^2$	$k_h$ (g mg <sup>-1</sup> min <sup>-1</sup> )	$q_e$ (mg/g)	$R^2$	$q_{e,exp.}$ (mg/g)	$K_p$ (mg/g min <sup>0.5</sup> )	C	$R^2$
40	0.045	26.000	0.964	0.00325	41.666	0.999	38.488	1.471	24.050	0.835
60	0.044	49.107	0.998	0.00106	52.500	0.998	53.024	2.647	26.550	0.909
80	0.037	63.117	0.997	0.00051	63.330	0.995	66.605	4.009	25.840	0.946
100	0.036	77.944	0.998	0.00010	75.000	0.997	76.326	5.176	24.260	0.916
120	0.041	80.554	0.998	0.00013	84.860	0.998	86.488	6.041	24.460	0.952

slope and intercept values. As demonstrated previously (Table 7), it could be concluded that the pseudo-second-order model has the highest correlation coefficient.

In all initial concentrations, straight lines with high correlation coefficient (0.995) were obtained. In addition, calculated  $q_e$  from pseudo-second-order model was compatible with experimental data. So, it could be concluded that the pseudo-second-order kinetic model expresses the adsorption process and it confirms that the controlling step of adsorption of Acid red 18 on the composite surface may be chemical adsorption. As can be seen in Table 7,  $K$  values decrease with the increase in initial dye concentration. In higher concentrations, competition of dye molecules to achieve the active sites is higher and the rate of adsorption will be lower.

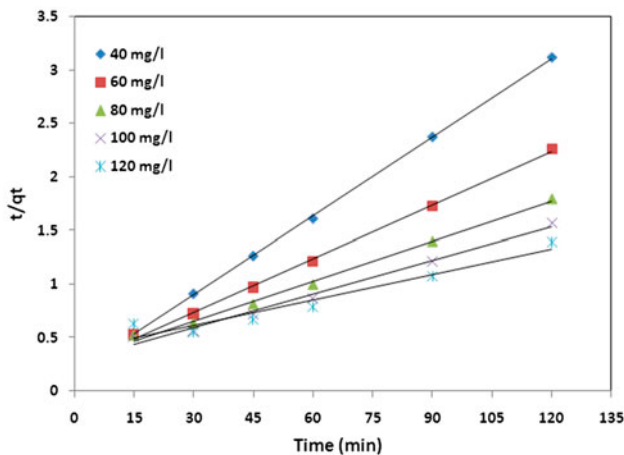


Fig. 12. Pseudo-second-order kinetic model for adsorption of Acid red 18 onto the composite at 25°C.

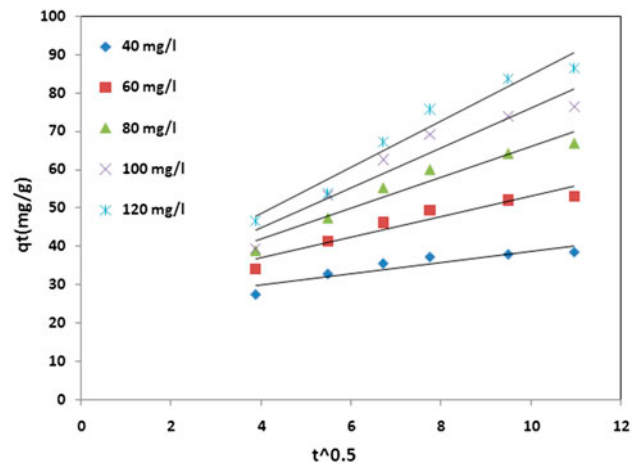


Fig. 13. Intra-particle diffusion model for adsorption of Acid red 18 onto polyaniline/HCl-MRH composite at 25°C.

### 3.9.3. Intra-particle diffusion model

This kinetic model is based on the model that was presented by Weber and Morris [38] where the diffusion model is expressed using the following equation:

$$q_t = k_p t^{0.5} + C \quad (11)$$

where  $C$  and  $k_p$  are the intercept and intra-particle diffusion rate constant (mg g<sup>-1</sup> min<sup>-0.5</sup>), respectively. In the Eq. (11),  $k_p$  is the slope of the line which is obtained from plotting  $q_t$  values (mg/g) vs.  $t^{0.5}$  and the intercept value indicates the boundary layer effects. With an increase in the intercept values, contribution of adsorption on the controlling step of the rate will increase. Table 7 demonstrates the values of  $k_p$  obtained from the findings of the present study. It reveals that the diffusion rate increases with the enhancement of initial dye concentration, which occurs due to the high driving force values and the

increase in  $C_0$ . If graphs from linear regression of  $q_t$  values against  $t^{0.5}$  pass through the origin, intra-particle diffusion is the only rate-controlling step. However, as demonstrated in Fig. 13, the linear graphs do not pass through the origin. Therefore, intra-particle diffusion is not the only rate-controlling step and other kinetic mechanisms may control the adsorption rate, which is proven with other studies of adsorption [39,40].

#### 4. Conclusion

In this study, useful adsorbent from low-cost agricultural waste such as rice husk was synthesized and performance of this adsorbent for the removal of Acid red 18 was evaluated. HCl-MRH was prepared from rice husk and the surface of HCl-MRH was functionalized by polyaniline. Polyaniline/HCl-MRH composite showed the highest performance for dye removal. Well-distributed polyaniline amine groups on the surface of HCl-MRH and increase in their amounts per unit area lead to the improvement in the composite ability for dye removal in comparison with HCl-MRH and polyaniline. It was observed that with the increase in pH, dye removal efficiency was reduced due to ionic effects. Polyaniline/HCl-MRH composite showed the higher dye removal efficiency in comparison with polyaniline and HCl-MRH at different pH. With the increase in the composite dosage up to 0.1 g, dye removal efficiency increased because of dye concentration gradient between the solution and the surface of composite, then no significant changes were seen. Due to the increase in adsorbent dosage and constant dye removal, adsorption capacity decreases. By studying the changes in the initial dye concentration, it was observed that dye removal decreased with the increase in dye concentration. To investigate the equilibrium adsorption, the contact time of 180 min in 40 ppm dye solution was evaluated. It was observed that after 120 min of contact, adsorption efficiency is constant and the equilibrium was achieved. Thermodynamic studies showed that temperature has a significant effect on dye removal. Percentage of dye removal increased with the increase in temperature, this is because of the increase in surface activity. The findings of thermodynamic study showed that the adsorption process is endothermic. Negative values of Gibbs free energy indicated that the adsorption process is spontaneous. Good conformity of experimental data with the isotherm models can be ranked based on  $R^2$  values as following:

Langmuir > Freundlich > Redlich–Peterson > Temkin > Dubinin–Radushkevich

Therefore, between all studied isotherms for the adsorption of Acid red 18 on composite, Langmuir model was the predominant model and expressed the monolayer adsorption on the surface of composite. According to kinetic studies, pseudo-second-order kinetic model is compatible with thermodynamic behavior of Acid red 18 adsorption on the surface of the composite at different dye concentrations.

#### References

- [1] Y.K. Chao, H.W. Chung, Y.W. Jane, Adsorption of direct dyes from aqueous solutions by carbon nanotubes: Determination of equilibrium, kinetics and thermodynamics parameters, *J. Colloid Interface Sci.* 327 (2008) 308–315.
- [2] Y. Yao, F. Xu, M. Chen, Z. Xu, Z. Zhu, Adsorption behavior of methylene blue on carbon nanotubes, *Bioresour. Technol.* 101 (2010) 3040–3046.
- [3] H.W. Chung, Adsorption of reactive dye onto carbon nanotubes: Equilibrium, kinetics and thermodynamics, *J. Hazard. Mater.* 144 (2007) 93–100.
- [4] J.L. Gong, B. Wang, G.M. Zeng, C.P. Yang, C.G. Niu, Q.Y. Niu, W.J. Zhou, Y. Liang, Removal of cationic dyes from aqueous solution using magnetic multi-wall carbon nanotube nanocomposite as adsorbent, *J. Hazard. Mater.* 164 (2009) 1517–1522.
- [5] Z. Aksu, I.A. Isoglu, Use of agricultural waste sugar beet pulp for the removal of Gemazol turquoise blue-G reactive dye from aqueous solution, *J. Hazard. Mater.* 137 (2006) 418–430.
- [6] M.H. Baek, C.O. Ijagbemi, O. Se-Jin, D.S. Kim, Removal of Malachite Green from aqueous solution using degreased coffee bean, *J. Hazard. Mater.* 176 (2010) 820–828.
- [7] B.H. Hameed, A.A. Ahmad, Batch adsorption of methylene blue from aqueous solution by garlic peel, an agricultural waste biomass, *J. Hazard. Mater.* 164 (2009) 870–875.
- [8] B.H. Hameed, M.I. El-Khaiary, Removal of basic dye from aqueous medium using a novel agricultural waste material: Pumpkin seed hull, *J. Hazard. Mater.* 155 (2008) 601–609.
- [9] V. Dulman, S.M. Cucu-Man, Sorption of some textile dyes by beech wood sawdust, *J. Hazard. Mater.* 162 (2009) 1457–1464.
- [10] P. Pengthamkeerati, T. Satapanajaru, O. Singchan, Sorption of reactive dye from aqueous solution on biomass fly ash, *J. Hazard. Mater.* 153 (2008) 1149–1156.
- [11] T. Akar, I. Tosun, Z. Kaynak, E. Ozkara, O. Yeni, E.N. Sahin, S.T. Akar, An attractive agro-industrial by-product in environmental cleanup: Dye biosorption potential of untreated olive pomace, *J. Hazard. Mater.* 166 (2009) 1217–1225.
- [12] A. Khaled, A. El-Nemr, A. El-Sikaily, O. Abdelwahab, Removal of Direct N Blue-106 from artificial textile dye effluent using activated carbon from orange peel: Adsorption isotherm and kinetic studies, *J. Hazard. Mater.* 165 (2009) 100–110.
- [13] N. Gupta, A.K. Kushwaha, M.C. Chattopadhyaya, Application of potato (*Solanum tuberosum*) plant wastes for the removal of methylene blue and

- malachite green dye from solution, *Arabian J. Chem.* (in press), doi: 10.1016/j.arabjc.2011.07.021.
- [14] Ö. Tunç, H. Tanacı, Z. Aksu, Potential use of cotton plant wastes for the removal of Remazol Black B reactive dye, *J. Hazard. Mater.* 163 (2009) 187–198.
- [15] M. Zabihi, A. Ahmadpour, A. Asl, Removal of mercury from water by carbonaceous sorbents derived from walnut shell, *J. Hazard. Mater.* 167 (2009) 230–236.
- [16] K. Nakagawa, A. Namba, S.R. Mukai, H. Tamon, P. Ariyadejwanich, W. Tanthapanichakoon, Adsorption of phenol and reactive dye from aqueous solution on activated carbons derived from solid wastes, *Water Res.* 38 (2004) 1791–1798.
- [17] K. Okada, N. Yamamoto, Y. Kameshima, A. Yasumori, Adsorption properties of activated carbon from waste newspaper prepared by chemical and physical activation, *J. Colloid Interface Sci.* 262 (2003) 194–199.
- [18] R.S. Juang, F.C. Wu, R.L. Tseng, Characterization and use of activated carbons prepared from bagasses for liquid-phase adsorption, *Colloids Surf. A: Physicochem. Eng. Aspects* 201 (2002) 191–199.
- [19] Y. Guo, S. Yang, W. Fu, J. Qi, R. Li, Z. Wang, H. Xu, Adsorption of malachite green on micro- and mesoporous rice husk-based active carbon, *Dyes Pigm.* 56 (2003) 219–229.
- [20] D. Kalderis, S. Bethanis, P. Paraskeva, E. Diamadopoulos, Production of activated carbon from bagasse and rice husk by a single-stage chemical activation method at low retention times, *Bioresour. Technol.* 99 (2008) 6809–6816.
- [21] Y. Chen, Y. Zhu, Z. Wang, Y. Li, L. Wang, L. Ding, Application studies of activated carbon derived from rice husks produced by chemical-thermal process—A review, *Adv. Colloid Interface Sci.* 163 (2011) 39–52.
- [22] M.A. Bavio, G.G. Acosta, T. Kessler, Synthesis and characterization of polyaniline and polyaniline-Carbon nanotubes nanostructures for electrochemical supercapacitors, *J. Power Sources* 245 (2014) 475–481.
- [23] H. Yan, K. Kou, Enhanced thermoelectric properties in polyaniline composites with polyaniline-coated carbon nanotubes, *J. Mater. Sci.* 49 (2014) 1222–1228.
- [24] M.M. Rahman, N. Akter, M.R. Karim, N. Ahmad, M.M. Rahman, I.A. Siddiquey, N.M. Bahadur, M.A. Hasnat, Optimization, kinetic and thermodynamic studies for removal of Brilliant Red (X-3B) using Tannin gel, *J. Environ. Chem. Eng.* 2 (2014) 76–83.
- [25] Q.Q. Zhong, Q.Y. Yue, Q. Li, X. Xu, B.Y. Gao, Preparation, characterization of modified wheat residue and its utilization for the anionic dye removal, *Desalination* 267 (2011) 193–200.
- [26] E. Binaeian, N. Seghatoleslami, M.J. Chaichi, Synthesis of oak gall tannin-immobilized hexagonal mesoporous silicate (OGT-HMS) as a new super adsorbent for the removal of anionic dye from aqueous solution, *Desalin. Water Treat.* 57 (2016) 8420–8436.
- [27] H.A. Tayebi, Z. Dalirandeh, A. Shokuhi Rad, A. Mirabi, E. Binaeian, Synthesis of polyaniline/Fe<sub>3</sub>O<sub>4</sub> magnetic nanoparticles for removal of reactive red 198 from textile waste water: Kinetic, isotherm, and thermodynamic Studies, *Desalin. Water Treat.* (2016) 1–13, doi: 10.1080/19443994.2015.1133323.
- [28] P. Senthil Kumar, S. Ramalingam, C. Senthamarai, M. Niranjanaa, P. Vijayalakshmi, S. Sivanesan, Adsorption of dye from aqueous solution by cashew nut shell: Studies on equilibrium isotherm, kinetics and thermodynamics of interactions, *Desalination* 261 (2010) 52–60.
- [29] H.A. Tayebi, M.E. Yazdanshenas, A. Rashidi, R. Khajavi, M. Montazer, The isotherms, kinetics and thermodynamics of acid dye on nylon 6 with different amounts of titania and fiber cross sectional shape, *J. Eng. Fiber Fabr.* 10 (2015) 97–108.
- [30] N.A. Kamal, Removal of direct blue-106 dye from aqueous solution using new activated carbons developed from pomegranate peel: Adsorption equilibrium and kinetics, *J. Hazard. Mater.* 165 (2009) 52–62.
- [31] Ö. Tunç, H. Tanacı, Z. Aksu, Potential use of cotton plant wastes for the removal of Remazol Black B reactive dye, *J. Hazard. Mater.* 163 (2009) 187–198.
- [32] B.H. Hameed, Spent tea leaves: A new non-conventional and low-cost adsorbent for removal of basic dye from aqueous solutions, *J. Hazard. Mater.* 161 (2009) 753–759.
- [33] M.J. Temkin, V. Pyzhev, Recent modifications to Langmuir isotherms, *Acta Physicochim. URSS.* 12 (1940) 217–225.
- [34] M. Wawrzekiewicz, Sorption of Sunset Yellow dye by weak base anion exchanger—Kinetic and equilibrium studies, *Environ. Technol.* 32 (2011) 455–465.
- [35] T.L. Seey, M.J.N.M. Kassim, Acidic and basic dyes removal by adsorption on chemically treated mangrove barks, *Int. J. Appl. Sci. Technol.* 2 (2012) 270–276.
- [36] M. Ghaedi, Comparison of cadmium hydroxide nanowires and silver nanoparticles loaded on activated carbon as new adsorbents for efficient removal of Sunset yellow: Kinetics and equilibrium study, *Spectrochim. Acta Part A: Mol. Biomol. Spectrosc.* 94 (2012) 346–351.
- [37] W. Li, Y. Tang, Y. Zeng, Z. Tong, D. Liang, W. Cui, Adsorption behavior of Cr(VI) ions on tannin-immobilized activated clay, *Chem. Eng. J.* 193–194 (2012) 88–95.
- [38] W.J. Weber, J.C. Morris, Kinetics of adsorption on carbon from solution, *J. Sanit. Eng. Div. Am. Soc. Civ. Eng.* 89 (1963) 31–60.
- [39] J. Sanchez-Martin, M. Gonzalez-Velasco, J. Beltran-Heredia, J. Gragera-Carvajala, J. Salguero-Fernandez, Novel tannin-based adsorbent in removing cationic dye (Methylene Blue) from aqueous solution. Kinetics and equilibrium studies, *J. Hazard. Mater.* 174 (2010) 9–16.
- [40] Sumanjit, S. Rani, R.K. Mahajan, Equilibrium, kinetics and thermodynamic parameters for adsorptive removal of dye Basic Blue 9 by ground nut shells and Eichhornia, *Arabian J. Chem.* (in press), doi: 10.1016/j.arabjc.2012.03.013.